



VOLUME 63 | 2014

journal homepage: http://journalofenergy.com/

Leonardo Štrac Končar Power Transformers Ltd. leonardo.strac@siemens.com Franjo Kelemen Končar Power Transformers Ltd. franjo.kelemen@siemens.com

Magnetizing current of a Large Power Transformer and its Harmonic Spectrum in Normal and GIC conditions

SUMMARY

A measurement of the harmonic spectrum of magnetizing current was performed. This paper analyzes the results of the measurement of harmonic spectrum of magnetizing current in standard no-load test at various values of induction. Magnetizing current harmonic spectrum during single-phase no-load test was measured as well as the impact of combined AC and DC magnetization on core behavior and harmonic spectrum. A mathematical model of transformer core is introduced. The calculated results are presented.

Key words: power transformer, no load condition, magnetizing current, harmonic spectrum, geomagnetically-induced currents

1. INTRODUCTION

Dealing with apparent power and power factor in distribution systems is the standard part of everyday maintenance. There are many sources of higher harmonics in the system: wind farms, power convertors, SVC and nonlinear elements, such as power transformers. Also, in some countries on far north and south like Canada or South Africa the possibility of geomagnetically-induced currents (GIC) due to solar storms are high. To broaden knowledge of power transformer core behavior on distribution system and impact of GIC on transformers core magnetizing current, Končar Power Transformers (KPT) conducted a series of special measurements on a five-limb core. The harmonic spectrum of magnetizing current in standard noload test at various values of induction in the core is analyzed. Additionally, magnetizing current harmonic spectrum during single-phase no-load test was considered and the impact of combined AC and DC magnetization on core behavior and harmonic spectrum. The measurements are compared with simulation results.

2. MEASUREMENT SETUP

The measurement of transformer core behavior and properties under special conditions was conducted at KPT. The test model was the three-phase five-limb core outside of tank equipped with custom-made temporary windings. Beside standard three-phase no load test and single phase no load test, the test setup included GIC injection. For this purpose, the special arrangement of the test windings was used to allow the possibility of simultaneous AC and DC magnetization of the core. Number of turns on both AC and DC winding is 39. AC potential is also induced in DC winding, but since DC source is located in one point of delta connection of windings there is no AC potential on DC source.



Figure 1 - Custom-made temporary windings during measurements

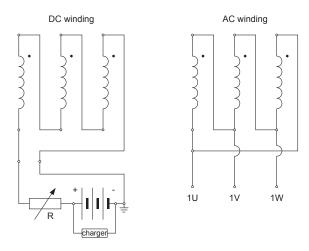


Figure 2 - Electrical schematic of DC and AC winding

3. MATHEMATICAL MODEL

The magnetic circuit model of a five-limb transformer core is derived using some usual assumptions and approximations.

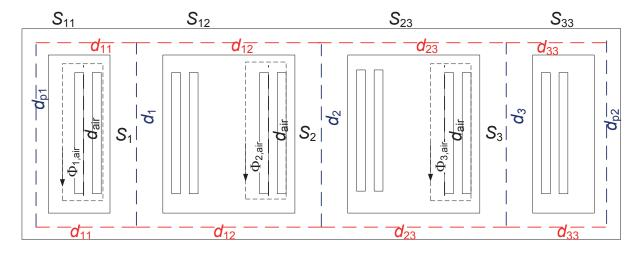


Figure 3 - Simplified schematic of a five - limb core cross section and winding arrangement.

Using the notation established in the Fig. 3, the system of equations (1)-(10) that describes the behavior of the magnetic circuit can be formed.

$$N(I_{o1}(t) + I_{DC1}) = H_1 d_1 + H_{11}(2d_{11} + d_{11})$$
(1)

$$N(I_{o1}(t) - I_{o2}(t) + I_{DC1} - I_{DC2}) = H_1 d_1 + 2H_{12} d_{12} - H_2 d_1$$
 (2)

$$N(I_{o2}(t) - I_{o3}(t) + I_{DC2} - I_{DC3}) = H_2 d_1 + 2H_{23} d_{23} - H_3 d_3$$
(3)

$$N(I_{o3}(t) + I_{DC3}) = H_3 d_3 + H_{33}(2d_{33} + d_{n2})$$
(4)

$$N(I_{o1}(t) + I_{DC1}) = H_{1 air} d_{air}$$
(5)

$$N(I_{o2}(t) + I_{DC2}) = H_{2 air} d_{air}$$
(6)

$$N(I_{o3}(t) + I_{DC3}) = H_{3 \text{ air}} d_{air}$$
(7)

$$0 = \mu_0 \mu_{r1}(H_1) H_1 S_1 - \mu_0 \mu_{r11}(H_{11}) H_{11} S_{11} - \mu_0 \mu_{r12}(H_{12}) H_{12} S_{12} - \mu_0 H_{1 air} S_{air}$$
 (8)

$$0 = \mu_0 \mu_{r2}(H_2) H_2 S_2 + \mu_0 \mu_{r12}(H_{12}) H_{12} S_{12} - \mu_0 \mu_{r23}(H_{23}) H_{23} S_{23} - \mu_0 H_{2,air} S_{air}$$
 (9)

$$0 = \mu_0 \mu_{r3}(H_3) H_3 S_3 + \mu_0 \mu_{r23}(H_{23}) H_{23} S_{23} - \mu_0 \mu_{r33}(H_{33}) H_{33} S_{33} - \mu_0 H_{3,air} S_{air}$$
 (10)

In equations (1)-(10) N denotes number of turns of the excited winding, IO1 the alternating part of magnetizing current of the first phase, IDC1 the direct current in phase 1, H1 is the magnetic field strength and the index is given according to the geometric path in Fig. 1, d is the geometric length with index corresponding to the path leg according to Fig. 1, t is the time variable, μ_0 is the magnetic permeability of the vacuum, ur is relative permeability of the material followed with the index corresponding to path in Fig. 1, numbered indices 1,2,3 given to currents represent three phases of a transformer, while S represents the cross-section area of the path leg according to Fig. 1. Additional equations are obtained using the fact that the system is powered by a three-phase symmetric system of voltages without harmonic distortion. This means that the magnetic flux linkage of the windings with respect to the time variable is also a harmonic function satisfying

$$V_1 \sin(\omega t) = N \frac{\mathrm{d}\Phi_1}{\mathrm{d}t} \Longrightarrow \Phi_1(t) = \frac{-V_1 \cos(\omega t)}{\omega N} + \Phi_{1DC},$$
 (11)

where V1 denotes the amplitude of the applied voltage to the first phase of a transformer, ω is the angular frequency of the voltage, and Φ1DC is an integration constant representing the DC component of flux resulting from the DC current magnetization. Similar relations hold for the other two phases (denoted with indices 2 and 3, respectively), so the following three equations (12)-(14) complete the system of equations needed for the full mathematical description of a model.

$$\frac{-V_1 \cos(\omega t)}{\omega N} + \Phi_{1DC} = \mu_0 \mu_{r1}(H_1) H_1 S_1$$
 (12)

$$\frac{\omega N}{-V_1 \cos\left(\omega t - \frac{2\pi}{3}\right)} + \Phi_{2DC} = \mu_0 \mu_{r_2}(H_2) H_2 S_2$$

$$\frac{-V_1 \cos\left(\omega t - \frac{4\pi}{3}\right)}{\omega N} + \Phi_{3DC} = \mu_0 \mu_{r_3}(H_3) H_3 S_3$$
(14)

$$\frac{-V_1 \cos\left(\omega t - \frac{4\pi}{3}\right)}{\omega N} + \Phi_{3DC} = \mu_0 \mu_{r3}(H_3) H_3 S_3$$
 (14)

The magnetic behavior of the core in reality is very complex because the super oriented steel sheets are both anisotropic, and nonlinear. For the purpose of this paper, the anisotropic behavior of the material is neglected, which is equivalent to the assumption that all the magnetic flux lines coincide with the rolling direction of the steel. The nonlinear B-H curve is modeled using the simple relationship between the two field vector amplitudes and without incorporating hysteresis.

Based on the mathematical model described in this section, three series of calculations were done. The first one was to calculate (average) harmonic content of the no load current for AC magnetization of the core on different induction levels (induced voltages). The curves describing the harmonic content expressed as the percentage of the first harmonic rise with induction, and then fall off because of the influence of the active current covering the losses inside the core (Figure 4). Cases with constant DC current and variable induction, as well as the case with variable DC and "constant" induction are given in Figures 5-6. Qualitative behavior of the harmonics corresponds well to the measurements. It is important to notice that the calculated values are given as arithmetic averages of the phases. Each phase has its own signature harmonic content, which varies significantly from phase to phase. This is why the analysis should be taken as a qualitative prediction of the transformer behavior. Especially because the measurements cannot directly express the magnetizing current, but the resulting vector sum current from the active part covering the losses, magnetizing current etc. Therefore, the base harmonic differs from the one calculated using the magnetizing current only.

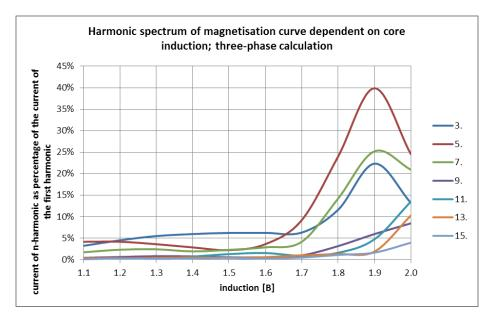


Figure 4 - Harmonic spectrum of magnetization curve dependent on core induction; three-phase calculation, phase current

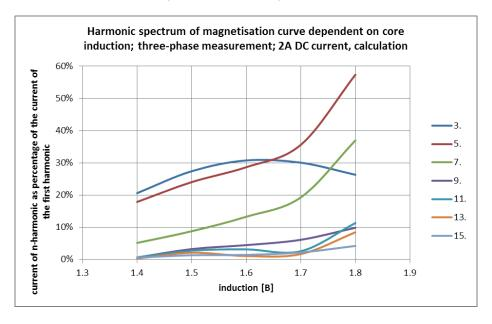


Figure 5 - Harmonic spectrum of magnetization curve dependent on core induction; 2A DC current calculation, phase current

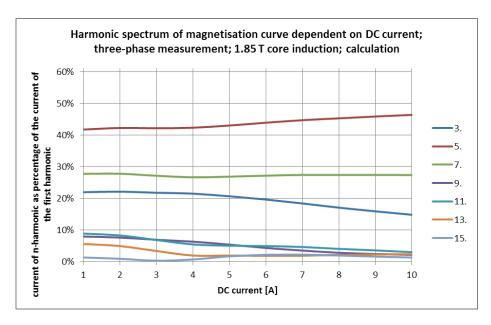


Figure 6 - Harmonic spectrum of magnetization curve dependent on DC current; 1,85 T core induction, calculation, phase current

4. MEASUREMENTS

4.1. Measurement Results for Three-Phase No Load Test

From the diagram in Figure 7 one can see that for typical working range of induction of power transformers (1.4 - 1.8 T) harmonics above the eleventh order are practically non-existent. However, thirteenth harmonic appears above the induction of 1.8 T, but only up to 5% of the first harmonic. Based on their behavior, it can be said that there are two groups of higher harmonics: the third harmonic in one group and all the others in second group. Share of the third harmonic remains rather constant (between 10% - 15%) through the range of induction, falling significantly above 1.8 T. Harmonics fifth and above increase their share constantly through the range of induction up to the saturation induction of 1.95 T when shares start to fall rapidly. Up to the induction of 1.6 T third harmonic is the dominant one, but above that higher harmonics start to dominate.

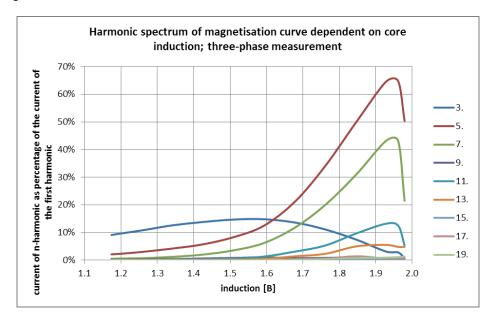


Figure 7 - Harmonic spectrum of magnetization curve dependent on core induction; three-phase measurement; phase current

4.2. Measurement Results for Single-Phase No Load Test

During the single-phase magnetization, only the limb that is magnetized can be saturated, while the other parts of the core distribute the flux through the much bigger area avoiding saturation. Since the harmonic distribution for geometrically equal limbs is practically the same, here is presented only the average values, rather than individual ones. In this situation, diagram of higher harmonics looks completely different. For all three main limbs the share of all harmonics rise linearly up to the saturation induction (Figure 8). Unlike for the three-phase magnetization, lesser the order of harmonic, higher the share of the harmonic, without line crossing.

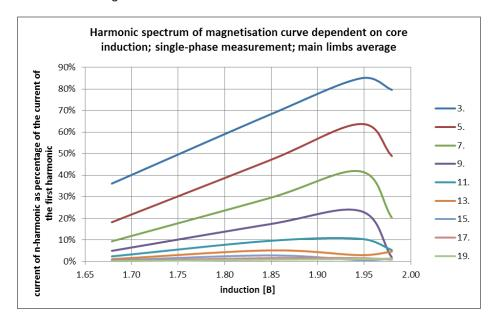


Figure 8 - Harmonic spectrum of magnetization curve dependent on core induction; single-phase measurement, phase current; main limbs average

4.3. Measurement Results for Combined AC and DC Magnetization

Although results apply to combined AC and DC magnetization, for the sake of comparison value of induction in diagrams are calculated for AC magnetization only.

Additional DC magnetization has a big impact on harmonic distribution even at only 2A DC (this correspond to 2×39=78 ampere turns). Third harmonic is 30% of the first harmonic which is twice as high as the share of the third harmonic without DC magnetization. Also, even at a low AC core induction of 1.34 T, core is saturated at 6A DC (this correspond to 6×39=234 ampere turns).

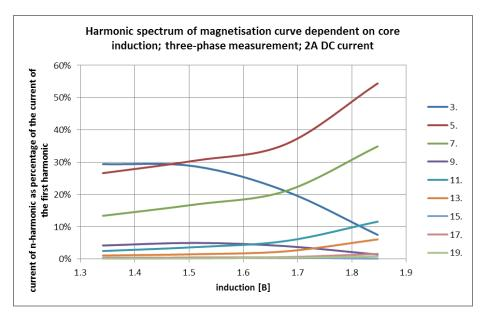


Figure 9 - Harmonic spectrum of magnetization curve dependent on core induction; three-phase measurement, phase current; 2A DC current

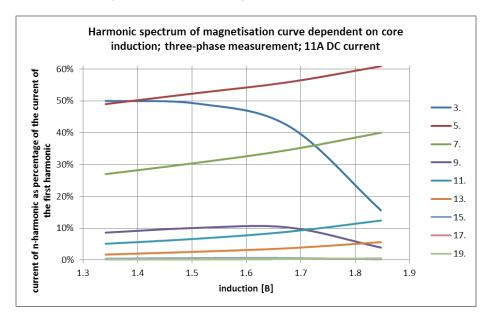


Figure 10 - Harmonic spectrum of magnetization curve dependent on core induction; three-phase measurement, phase current; 11A DC current

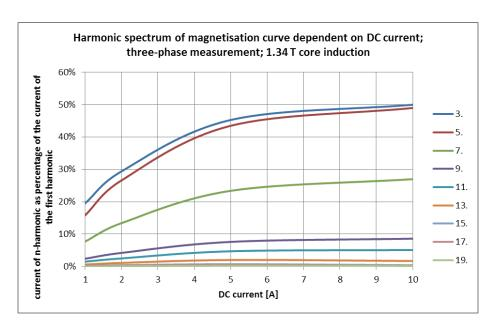


Figure 11 - Harmonic spectrum of magnetization curve dependent on DC current; three-phase measurement, phase current; 1.34 T core induction

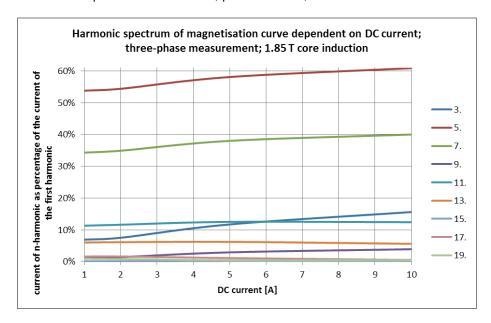


Figure 12 - Harmonic spectrum of magnetization curve dependent on DC current; three-phase measurement, phase current; 1.85 T core induction

7. CONCLUSION

Results calculated with mathematical model are qualitatively comparable with the measured ones. Precise calculation of harmonic distribution across the induction range is hard to achieve because of lack of transformers core magnetization curve. Besides that, mathematical model calculates only magnetizing current and only the total no load current which consists from magnetizing current, losses current and winding capacitance current.

Measurement results for three-phase no load test shows that for typical working range of induction of power transformers (1.4 - 1.8 T) harmonics above the eleventh order are practically non-existent. Dominant harmonics are third, fifth, seventh and ninth. Measurement also shows that harmonic share is highly dependable on core induction.

During the single-phase magnetization diagram of higher harmonics looks completely different. For main limbs the share of all harmonics rise linearly up to the saturation induction. Unlike for the three-phase magnetization, lesser the order of harmonic, higher the share of the harmonic, without line crossing.

Additional DC magnetization has a big impact on harmonic distribution even at only 2A DC (this correspond to 78 ampere turns). Third harmonic is 30% of the first harmonic which is twice as high as the share of the third harmonic without DC magnetization. Also, even at a low AC core induction of 1.34 T, core is saturated at 6A DC (this correspond to 234 ampere turns).

5. REFERENCES

- [1] F. Kelemen, L. Štrac, Impact of geomagnetically induced currents on magnetizing currents under no-load conditions, International Colloquium Transformer Research and Asset Management, Cavtat, Croatia, November 12-14, 2009
- [2] L. Štrac, F. Kelemen, Istraživanje utjecaja geomagnetski induciranih struja na energetske transformatore s trostupnom i peterostupnom jezgrom, 7. savjetovanje HO CIGRÉ, Cavtat, Croatia, November 06-10, 2005